

# Description of high energy $\pi N$ -scattering data by the complex Regge pole model

M. I. Dzhgarkava, Yu. M. Kazarinov, I. K. Potashnikova, and I. N. Silin

Joint Institute for Nuclear Research

(Submitted April 22, 1974)

Zh. Eksp. Teor. Fiz. 67, 839-847 (September 1974)

The available experimental data on  $\pi N$  elastic scattering and charge exchange are analyzed within the framework of the complex Regge pole model. The results of experiments with energies above 10 GeV at momentum transfers up to 1 GeV/c are employed (a total of 802 experimental points). Statistically satisfactory agreement with the experiments (confidence level C.L.  $\approx 0.63\%$ ) is obtained by taking exchange of the  $p$ ,  $p'$ ,  $\rho$ , and  $\rho'$  trajectories.

A statistically satisfactory description of the experimental data on  $\pi N$  scattering in the energy region  $p_L \geq 10$  GeV/c in the momentum-transfer interval  $0.01 \leq |t| \leq 1.00$  (GeV/c)<sup>2</sup> was obtained earlier in [1] on the basis of a quasipotential approach. The predictions based on this approach were confirmed by measurements of the polarization parameters in  $\pi^+p$  scattering [2] and of the differential cross section [3] in elastic  $\pi^+p$  scattering and scattering with charge exchange (see Figs. 1-5, dashed curves).

For a correct comparison of the quasipotential approach with the theory of complex angular momenta, it would be of interest to carry out an analogous reduction of the experimental data in the energy region indicated above, using the model of complex angular momenta. It was shown earlier that the use of the pure pole variant of this model yields only a qualitative description of the experiment and accounts well for only a number of general properties of hadron scattering at high energies [4-6]. It was shown in [7], however, that allowance for the moving branch points generated in the  $j$  plane by Regge poles may turn out to be quite significant for the description of the scattering of particles at high energies. We present below the results of an analysis of the known experimental data, based on one variant of the theory of complex angular momenta, in which branch points in the  $j$ -plane are taken into account.

At present there are several variants of models containing the contributions of the branch points. The most widely used in the literature are branch points due to rescattering. Their contribution and the contributions of the poles enter in the scattering amplitude additively, and the  $t$ -channel partial amplitude takes the form

$$T(t, j) = \frac{A(t, j)}{j - \alpha_p(t)} + B(t, j) \ln[j - \alpha_c(t)],$$

where  $\alpha_p(t)$  and  $\alpha_c(t)$  are the trajectories of the poles and of the branch point. A reduction of the experimental data on the basis of this model was carried out, for example, in [8, 9]. It is known, however, from the work of Ter-Martirosyan and co-workers it is known that a satisfactory description of the data is obtained only in the interval  $|t| \leq 0.5$  (GeV/c)<sup>2</sup> ( $\chi^2/N = 1.1$ , where  $N$  is the number of experimental points [8]). Thus, the model used in [8] does not make it possible to describe the experimental data in the interval of  $t$  of interest to us. In this connection, another possibility on the appearance of branch points in the  $j$  plane was considered.

In a number of models, allowance for the branch points

leads to the following expression for the partial amplitude:

$$T(t, j) = \frac{N}{[j - \alpha_p(t)] + \epsilon f [j - \alpha_c(t)]}.$$

In the available theoretical papers, two types of singularities are considered: logarithmic ( $f \propto \ln[j - \alpha_c(t)]$ ) and square-root ( $f \propto [j - \alpha_c(t)]^{1/2}$ ) [10, 11]. Zachariassen and his co-workers [12] have shown that when the amplitude has such a structure a pair of complex conjugate poles is produced at negative  $t$  when the pole trajectories and the branch points intersect in the complex  $j$  plane.

The analysis of the experimental data, performed so far within the framework of this model, was only illustrative in character [10, 13, 14]. An attempt at systematically describing a large amount of experimental data [15] has led only to qualitative agreement between theory and experiment ( $\chi^2/N = 2.5$  at  $N = 358$ ). Nonetheless, it can be concluded on the basis of these papers that the qualitative description does not depend strongly on the form of the branch point. Therefore, for the sake of simplicity, we have considered a square-root cut, all the more since the use of the square-root cut has enabled us to describe well the charge-exchange process [10, 14]. In addition, there was reason for hoping that allowance for  $\rho'$ -trajectory exchange will improve the agreement between the model and experiment in the interval  $0.01 \leq |t| \leq 1.0$  (GeV/c)<sup>2</sup>.

Unfortunately, in the customarily employed approximation, this model is valid only in a limited energy reg-

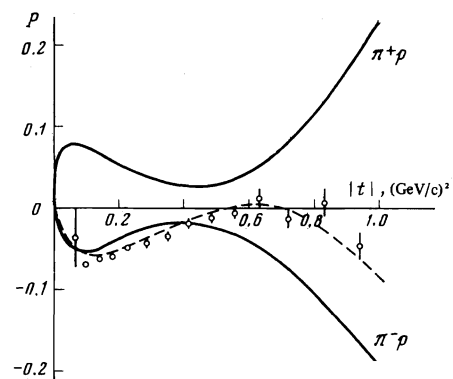


FIG. 1. Comparison of the predictions for the polarization with the experimental results in  $\pi^+p$  scattering [2]. Solid curves—prediction based on the Regge-pole model, dashed—with the aid of the quasipotential approach.  $p_L = 40$  GeV/c.

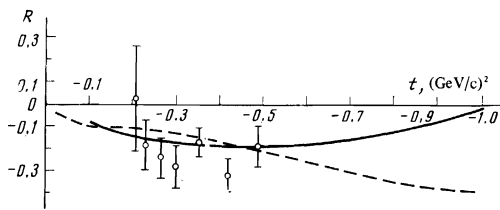


FIG. 2. Comparison of the predictions for the Wolfenstein parameter  $R$  with the result of experiment in  $\pi^-p$  scattering [2]. Solid curve—prediction made on the basis of the Regge-pole model, dashed—with the aid of the quasipotential approach.

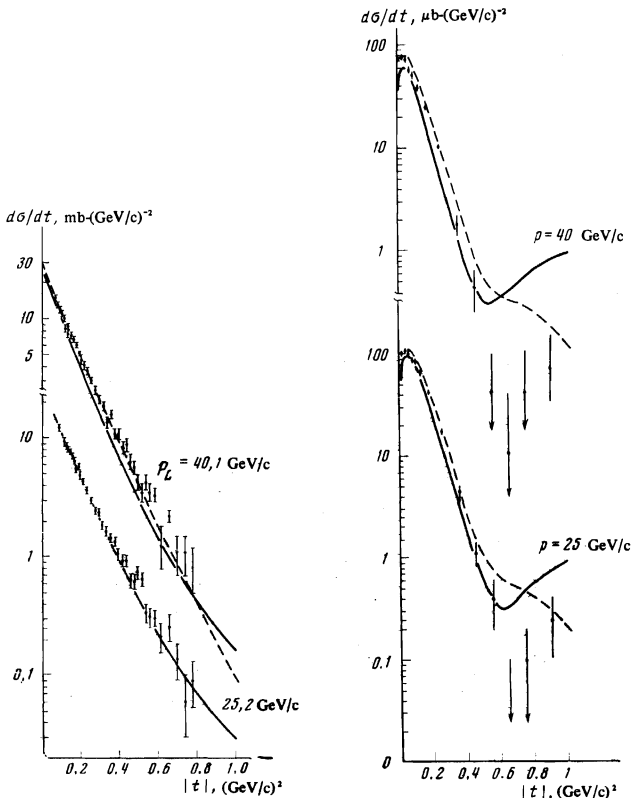


FIG. 3

FIG. 4

FIG. 3. Comparison of the predictions for the differential cross sections for the results of experiments on  $\pi^-p$  scattering [3]. Solid curve—prediction based on the Regge-pole model, dashed—with the aid of the quasipotential approach.

FIG. 4. Comparison of the predictions for the differential cross sections with the results of experiments in the reaction  $\pi^-p \rightarrow \pi^0n$ . Solid curve—prediction based on the Regge-pole model, dashed—with the aid of the quasipotential approach.

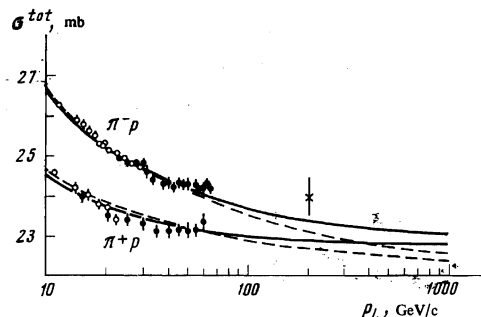


FIG. 5. Comparison of the predictions for the total cross sections with the results of experiments in  $\pi^-p$  scattering [3]. Solid curve—prediction based on the Regge-pole model, dashed—with the aid of the quasipotential approach.

ion [13]. Estimates show [15] that the upper limit does not exceed in this case 30 GeV.

## 1. $\pi$ N-SCATTERING AMPLITUDE

The  $\pi$ N-scattering amplitude is written in the form

$$M(s, t) = M_0 + M_1(\sigma_n),$$

where  $M_0$  and  $M_1$  are respectively the amplitudes without and with spin flip, and are determined by the sums of amplitudes corresponding to exchange of different reggeons:

$$M_0 = \sum_a M_{0a}, \quad M_1 = \sum_a M_{1a}.$$

We assume that the exchange of the  $p$ ,  $p'$ ,  $\rho$ , and  $\rho'$  trajectories predominates in the  $t$  channel. Then

$$M(\pi^-p) = M_p + M_{p'} + M_\rho + M_{\rho'}, \quad M(\pi^+p) = M_p + M_{p'} - M_\rho - M_{\rho'}, \\ M(\pi^-p \rightarrow \pi^0n) = \sqrt{2}(M_\rho + M_{\rho'}).$$

In the considered complex-pole model [13], the amplitude  $M_a$  for the exchange of the reggeon  $a$  is a sum of contributions of two complex-conjugate poles with trajectories  $\alpha_a(t)$  and  $\alpha_a^*(t)$ , and an integral along the cut corresponding to the branch point  $\alpha_a^C(t)$  (we shall henceforth omit the subscript  $a$  of  $\alpha$ ):

$$M_a(s, t) = \beta_+ S^{\alpha^+(t)} + \beta_- S^{\alpha^-(t)} + \int_{-\infty}^{\alpha^C(t)} T(t, j) S^{j-1} dj,$$

where  $\alpha^+(t) = \alpha^-(t)^*$ .

It was shown in [13] that this complicated picture in a limited energy interval at small  $\text{Im } \alpha(t)$  can be effectively represented by a pair of two complex conjugate poles:

$$M_a(s, t) = \beta_+ S^{\alpha^+} + \beta_- S^{\alpha^-}.$$

Then the amplitude for the exchange of one reggeon can be expressed in the form

$$M_{0a} = \gamma_{+a}^0(t) \eta_{+a}(E/E_0)^{\alpha^+(t)-1} + \gamma_{-a}^0(t) \eta_{-a}(E/E_0)^{\alpha^-(t)-1}, \\ M_{1a} = (\gamma_{+a}^1(t) \eta_{+a}(E/E_0)^{\alpha^+(t)-1} + \gamma_{-a}^1(t) \eta_{-a}(E/E_0)^{\alpha^-(t)-1}) \sqrt{-t/2m_N}, \\ \eta_{\pm a} = -[1 + \sigma_a \exp\{-i\pi\alpha(t)\}] / \sin \pi\alpha^\pm(t), \\ \alpha^\pm(t) = \alpha_0 + \alpha'(t) \pm i\alpha_1 \sqrt{-t},$$

where  $\eta_a$  is the signature factor, with  $\sigma_a = 1$  for the  $p$  and  $p'$  trajectories, and  $\sigma_a = -1$  for the  $\rho$  and  $\rho'$  trajectories;  $E_0 = 1$  GeV and  $m_N$  is a nucleon mass.

In the limiting case when  $\text{Im } T(t, j) \rightarrow 0$ , the cut van-

TABLE I

| $p_L$ , GeV/c | Number of points N | $\Delta x^2/N$ | Norms                             | $p_L$ , GeV/c | Number of points N | $\Delta x^2/N$ | Norms                             |
|---------------|--------------------|----------------|-----------------------------------|---------------|--------------------|----------------|-----------------------------------|
|               |                    |                | $\frac{d\sigma}{dt}(\pi^-p)$ [16] |               |                    |                | $\frac{d\sigma}{dt}(\pi^+p)$ [16] |
| 9.84          | 9                  | 0.86           | 0.991±0.014                       | 9.86          | 9                  | 0.98           | 1.019±0.019                       |
| 9.89          | 12                 | 0.69           | 0.987±0.010                       | 10.02         | 12                 | 0.35           | 0.987±0.007                       |
| 10.80         | 14                 | 2.29           | 0.905±0.023                       | 10.8          | 15                 | 1.45           | 1.006±0.023                       |
| 11.89         | 11                 | 0.35           | 0.992±0.010                       | 11.95         | 15                 | 1.56           | 0.980±0.012                       |
| 12.4          | 20                 | 0.42           | 0.916±0.018                       | 12.4          | 19                 | 0.85           | 0.900±0.000                       |
| 13.0          | 13                 | 2.13           | 0.990±0.023                       | 12.8          | 14                 | 0.64           | 1.076±0.028                       |
| 14.16         | 11                 | 0.64           | 1.011±0.014                       | 14.0          | 12                 | 0.76           | 0.983±0.016                       |
| 14.84         | 8                  | 1.12           | 1.080±0.038                       | 14.8          | 13                 | 0.66           | 1.121±0.027                       |
| 15.0          | 13                 | 1.17           | 1.026±0.026                       | 16.02         | 18                 | 1.10           | 1.020±0.009                       |
| 15.99         | 14                 | 0.23           | 0.989±0.008                       | 16.7          | 13                 | 1.57           | 1.113±0.030                       |
| 16.0          | 16                 | 0.34           | 0.979±0.007                       | 17.96         | 17                 | 0.76           | 0.983±0.013                       |
| 17.0          | 12                 | 0.67           | 1.054±0.027                       | 20.19         | 17                 | 0.67           | 0.979±0.017                       |
| 18.19         | 14                 | 0.49           | 1.029±0.007                       |               |                    |                | $\frac{d\sigma}{dt}(\pi^0n)$ [16] |
| 18.4          | 15                 | 0.22           | 1.135±0.029                       | 9.8           | 14                 | 1.03           | 1.015±0.045                       |
| 18.9          | 6                  | 0.41           | 1.135±0.048                       | 10.0          | 7                  | 0.53           | 0.968±0.062                       |
| 19.75         | 7                  | 0.83           | 1.286±0.035                       | 13.3          | 13                 | 1.07           | 1.114±0.042                       |
| 20.15         | 17                 | 0.24           | 1.006±0.009                       | 13.3          | 10                 | 0.91           | 1.114±0.042                       |
| 20.38         | 18                 | 0.54           | 0.993±0.006                       | 18.2          | 13                 | 0.55           | 1.086±0.059                       |
| 22.43         | 19                 | 0.81           | 1.014±0.008                       | 18.2          | 9                  | 0.34           | 1.086±0.059                       |
| 23.18         | 7                  | 0.85           | 1.334±0.039                       |               |                    |                |                                   |
| 24.22         | 19                 | 0.78           | 1.023±0.008                       |               |                    |                |                                   |
| 25.34         | 8                  | 0.75           | 1.338±0.043                       |               |                    |                |                                   |
| 26.23         | 20                 | 1.62           | 1.015±0.007                       |               |                    |                |                                   |

TABLE II

| Measured quantity      | $p_L$ , GeV/c | $N$  | $\Delta\chi^2/N$ | Reference | Measured quantity | $p_L$ , GeV/c | $N$  | $\Delta\chi^2/N$ | Reference |
|------------------------|---------------|------|------------------|-----------|-------------------|---------------|------|------------------|-----------|
| $\sigma_{tot}(\pi^-p)$ | 10–28.68      | 27   | 0.47             | [16]      | $P(\pi^+p)$       | 14.0          | 7    | 1.18             | [16]      |
|                        | 21–65         | 19   | 1.32             | [17]      |                   | 40.0          | 15   | 1.16             | [19]      |
|                        | 9.84–22.1     | 30   | 1.2              | [16]      |                   | 14.0          | 19   | 0.92             | »         |
| $\sigma_{tot}(\pi^+p)$ | 15–60         | 10   | 2.47             | [18]      | $P(\pi^0n)$       | 17.5          | 8    | 0.88             | »         |
|                        | 10.0          | 15   | 1.82             | [16]      |                   | 8.0           | 6    | 3.47             | »         |
|                        | 12.0          | 13   | 1.93             | »         |                   | 11.2          | 7    | 1.03             | [20]      |
| $P(\pi^-p)$            | 10.0          | 21   | 0.91             | [19]      | $\alpha(\pi^-p)$  | 9.84–26.23    | 11   | 1.23             | [21]      |
|                        | 14.0          | 19   | 2.03             | »         |                   | 9.86–20.19    | 7    | 1.4              | »         |
|                        | 14.0          | 6    | 0.80             | [16]      |                   | $R(\pi^-p)$   | 16.0 | 8                | 0.93      |
| 12.0                   | 5             | 1.17 | »                |           |                   |               |      |                  |           |

ishes and we have one pole, the residue being real in this case. Since the model in question is based on the assumption that  $\text{Im } T(t, j)$  is small [13], to reduce the number of parameters the functions  $\gamma_a(t)$  were chosen to be real and were parametrized in the form

$$\gamma_{\pm a}^{\pm}(t) = \gamma_{\pm a}^{\pm}(t) = \gamma_{0, \pm}^{\pm} / [1 + (R_{0, \pm})^2 |t|]^2,$$

where  $\gamma_{0, \pm}^{\pm}$  and  $R_{0, \pm}^{\pm}$  are free parameters.

## 2. COMPARISON WITH EXPERIMENT

We analyzed the following experimental data (see Tables I and II): the total interaction cross sections

$$\sigma_{tot}(s) = 8\pi \text{Im } M_0(s, 0),$$

the differential cross sections

$$\frac{d\sigma}{dt}(t, s) = 4\pi (|M_0|^2 + |M_1|^2),$$

the polarization

$$P(t, s) = 2 \text{Im } (M_0 M_1^*) / (|M_0|^2 + |M_1|^2),$$

The Wolfenstein parameter

$$R = (|M_0|^2 - |M_1|^2) \cos \alpha - 2 \text{Re } (M_0 M_1^*) \sin \alpha / (|M_0|^2 + |M_1|^2),$$

and the masses of the resonances  $f$ ,  $f'$ ,  $\rho$ ,  $g$ ,  $T$ , and  $\rho'$ . We reduced altogether 802 points in the momentum interval  $10 \leq p_L \leq 65$  GeV/c and  $0.01 \leq |t| \leq 1$  (GeV/c)<sup>2</sup>. The bulk of the experimental data was concentrated in this case in the region  $p_L \leq 30$  GeV/c. For  $p_L > 30$  GeV/c we used only the data on the total cross sections, since there is no limitation on the energy interval in the case of the total cross sections.

The parameters that enter in the expression for the amplitudes were determined by least squares. To this end we minimized the functional

$$\chi^2 = \sum_{n,i} [F_i^k - M_n F_i^k(x_n)]^2 / (\sigma_i^k)^2,$$

where  $F_i^k$  is the experimental value of the quantity  $F$  measured at the  $i$ -th point of the  $k$ -th experiment;  $F_i^k(x_{10})$  is the calculated value of  $F_i^k$  from specified values of the parameters  $x_n$ ;  $\sigma_i^k$  is the error in the experimental value of  $F_i^k$ ;  $M_k$  is the norm of the  $k$ -th experiment. The norms were introduced to take into account the possible systematic errors that lead to a relative shift of the  $d\sigma/dt$  curves measured in different experiments.

The contribution made to the amplitude by each

TABLE III

| Trajectory | $\alpha_0$        | $\alpha'$         | $\alpha_{\text{Im}}$ |
|------------|-------------------|-------------------|----------------------|
| $p$        | 1                 | $0.584 \pm 0.011$ | —                    |
| $p'$       | $0.303 \pm 0.007$ | $0.741 \pm 0.004$ | $0.274 \pm 0.021$    |
| $\rho$     | $0.538 \pm 0.021$ | $0.900 \pm 0.005$ | $0.351 \pm 0.029$    |
| $\rho'$    | $0.649 \pm 0.031$ | $0.102 \pm 0.031$ | $0.448 \pm 0.012$    |

TABLE IV

| Trajectory | $\gamma_0$        | $R_0^2$             | $\gamma_1$         | $R_1^2$            |
|------------|-------------------|---------------------|--------------------|--------------------|
| $p$        | $2.331 \pm 0.005$ | $1.822 \pm 0.037$   | $13.234 \pm 3.918$ | $44.209 \pm 8.313$ |
| $p'$       | $1.378 \pm 0.05$  | $0.848 \pm 0.199$   | 0                  | 0                  |
| $\rho$     | $0.222 \pm 0.022$ | $8.8 \cdot 10^{-4}$ | $-4.544 \pm 0.427$ | $2.845 \pm 0.211$  |
| $\rho'$    | $0.051 \pm 0.012$ | $0.704 \pm 0.285$   | $0.095 \pm 0.019$  | $0 \pm 0.299$      |

reggeon, with the exception of the Pomeranchuk trajectory, contains seven parameters ( $\alpha_0$ ,  $\alpha'$ ,  $\alpha_i$ ,  $\gamma_0$ ,  $R_0^2$ ,  $\gamma_1$ , and  $R_1^2$ ). The Pomeranchuk trajectory was chosen to be real ( $\alpha_i = 0$ ) with a fixed value  $\alpha_0 = 1$ . Thus, we varied simultaneously 26 parameters. The experimental points that accidentally deviated from the calculated curves by three and more errors were eliminated from the reduction (15 out of a total of 802). For the obtained solution we got  $\chi^2 = 861$  at  $\bar{\chi}^2 = 761$  (confidence level C.L. = 0.65%). The corresponding parameters are given in Tables III and IV.

Thus, the complex-pole model in the approximation used by us makes it possible to describe the entire aggregate of the experimental data in the interval  $10 \leq p_L \leq 30$  GeV/c and  $0.01 \leq |t| \leq 1$  (GeV/c)<sup>2</sup> with the aid of 26 free parameters. It should be noted that the elimination of the imaginary parts of the trajectory ( $\alpha_{\text{Im}} = 0$ ) makes the description of the experimental data much worse, namely  $\chi^2$  increases to 1960 (C.L.  $\ll 10^{-6}$ ). On the other hand, if  $\rho$ -reggeon exchange is disregarded, then  $\chi^2$  increases to 1130 (C.L.  $\ll 10^{-6}$ ).

It is clear from Figs. 6 and 7, which are shown to illustrate the obtained description, that the calculated plots of the differential cross section and of the polarization are in fair agreement with experiment. As expected, the description becomes much worse at the boundaries of the indicated energy interval.

Figures 1–4 show a comparison of the predictions based on the obtained solution with results of later experiments [2,3] (solid curve). It is seen from the figures that within the limit of the energy region indicated above ( $p_L \leq 30$  GeV/c) there is good agreement between the predicted dependences and the experimental data. At higher energies, a noticeable discrepancy with experiment is observed in the region of large  $|t|$ . The dashed curves, which are the predictions based on the quasipotential approach [1], fit the experimental points much better in the region  $p_L > 30$  GeV/c.

The predictions obtained for the total cross sections in both models agree, within the limits of errors, with experiment up to  $p_L = 205$  GeV/c (Fig. 5).

Comparing the results obtained in this paper (C.L.  $\approx 0.65\%$ ) with the description in the quasipotential approach [1], we can state that the quasipotential approach yields a somewhat better result (C.L.  $\approx 2\%$ ). However, one must not attach too much significance to this difference, since the quality of the description in the employed complex-pole model can be improved somewhat by considering the more general case of complex residues, although this does increase the number of parameters.

It must also be emphasized that both models make it possible to describe the experiment with the aid of 26 free parameters only after renormalization of the experimental data against the differential data. The deviation of the norms from unity then greatly exceeds in some cases the systematic errors indicated by the authors of the experiments (see Tables I and II).

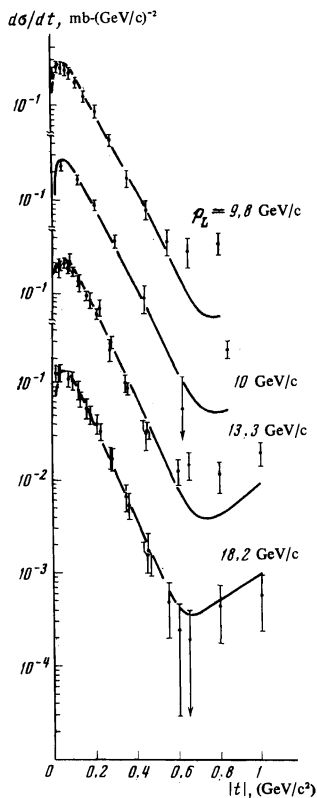


FIG. 6

FIG. 6. Differential cross section of the reaction  $\pi^-p \rightarrow \pi^0n$ .  
 FIG. 7. Polarization in the reaction  $\pi^-p \rightarrow \pi^0n$ .

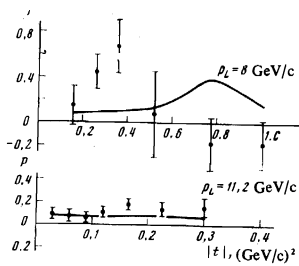


FIG. 7

- <sup>1</sup>M. I. Dzhgarkava, V. R. Garsevanishvili, S. V. Goloskokov, Yu. M. Kazarinov, V. A. Matveev, I. K. Potashnikova, I. N. Silin, and L. A. Slepchenko, JINR-preprint E2-6803, Dubna, 1973. Nucl. Phys., **B67**, 232, 1973.
- <sup>2</sup>C. Brunneton, J. Bystricky, G. Cozzika, J. Deregel, A. Derevschiko, Y. Ducros, A. Gaidot, Yu. Kazarinov, M. Kazarinov, V. Kanavets, B. Khatchaturov, F. Legar, A. De Lesonen, Yu. Mathlenko, J. P. Merlo, A. Mecshanian, S. Mijashita, I. Movchet, S. Nurushev, J. Pierrard, I. Potashnikova, G. Proskurin, L. van Rossum, A. Saraykin, V. Siksin, E. Smirnov, and V. Solovyanov. 2-nd-AIX-en-Provence International Conference on Elementary Particles, September, 1973.
- <sup>3</sup>Yu. M. Antipov, G. Ascoli, R. Busnello, G. Damgaard, M. V. Kienzle-Focacci, W. Kienzle, R. Klanner, L. G. Landsberg, A. A. Lebedev, C. Lechanoine, P. Lecomte, M. Martin, V. Roinishvili, R. D. Sard, A. Weitsch, and F. A. Yotch, Nucl. Phys. **B57**, 333 (1973); V. N. Bolotov, V. V. Isakov, D. B. Kakauridze, V. A. Kachanov, V. M. Kut'in, Yu. D. Prokoshkin, E. A. Razuvaev, V. K. Semenov, V. A. Sen'ko, and V. G. Rybakov, IFVÉ Preprint SEF 73-52; D. Bogert, R. Hanft, E. R. Huson, D. Ljung, C. Pascaud, S. Pruss, W. H. Smart, G. S. Pbrams, W. B. Fretter, C. E. Friedberg, G. Goldhaber, W. R. Graves, A. D. Johnson, J. A. Kadyk, L. Stutte, G. H. Trilling, F. C. Winkelmann, and G. P. Yost. NAL-Pub-73/57-EXP 7200.137.
- <sup>4</sup>K. T. Phillips, W. Rarita. Phys. Rev. **139B**, 1336 (1965).

- <sup>5</sup>V. A. Ter-Martirosyan, in: Voprosy fiziki elementarnykh chastits (Problems of Elementary Particle Physics), Erevan (1966), p. 479.
- <sup>6</sup>M. I. Dzhgarkava, Yu. M. Kazarinov, I. K. Potashnikova, and I. N. Silin, JINR Preprint R2-5320, Dubna (1970).
- <sup>7</sup>S. Mandelstam, Nuovo Cimento **30**, 1127, 1148 (1963); V. N. Gribov, I. Ya. Pomeranchuk, and K. A. Ter-Martirosyan, Yad. Fiz. **2**, 361 (1965) [Sov. J. Nucl. Phys. **2**, 258 (1966)].
- <sup>8</sup>K. G. Borekov, A. M. Lapidus, S. T. Sukhorukov, and K. A. Ter-Martirosyan, Yad. Fiz. **14**, 814 (1971) [Sov. J. Nuc. Phys. **14**, 457 (1972)].
- <sup>9</sup>R. C. Arnold and M. O. Blackman, Phys. Rev. **176**, 2082 (1968); S. Frautschi and B. Margolis, Nuovo Cimento **56A**, 1155 (1968); V. Yu. Gebov, A. B. Kaïdalov, S. T. Sukhorukov, and K. A. Ter-Martirosyan, Yad. Fiz. **10**, 1065 (1969) [Sov. J. Nucl. Phys. **10**, 609 (1970)]; A. Capella, J. Kaplan, A. Krzywicki, and D. Schiff, Nuovo Cimento **63A**, 141 (1969); F. Henyey, G. L. Kane, J. Pumplin, and M. H. Ross, Phys. Rev. **182**, 1579 (1969).
- <sup>10</sup>Bipin R. Desai, Peter Kaus, Robert T. Park, and F. Zachariassen, Phys. Rev. Lett. **25**, 1389, 1970.
- <sup>11</sup>D. Amati, S. Fubini, and A. Stanghellini, Nuovo Cim., **26**, 896, 1962. W. Frazer and C. Mehta, Phys. Rev. Lett. **23**, 258, 1969. G. F. Chew and D. R. Snider, Phys. Lett. **31B**, 75, 1970. R. C. Arnold, Phys. Rev. **140**, B1022, 1965. S. Frautschi and B. Margolis, Nuovo Cim., **56A**, 1155, 1968. R. Carlitz and M. Kislinger, Phys. Rev. Lett. **24**, 186, 1970.
- <sup>12</sup>P. Kaus and F. Zachariassen, Phys. Rev. **D1**, 2962, 1970. J. S. Ball and F. Zachariassen, Phys. Rev. Lett. **23**, 346, 1969.
- <sup>13</sup>J. S. Ball, G. Marchesili and F. Zachariassen, Phys. Lett. **31B**, 583, 1970.
- <sup>14</sup>N. P. Zotov and V. A. Tsarev, Yad. Fiz. **14**, 806 (1971) [Sov. J. Nucl. Phys. **14**, 453 (1972)].
- <sup>15</sup>R. T. Park, N. Barik, and D. T. Gregorich, Phys. Rev. **D6**, 3162, 1972.
- <sup>16</sup>G. Giacomelli, P. Pine, and S. Stagni, CERN, HERA 69-1, 1969.
- <sup>17</sup>S. P. Denisov, Yu. P. Dimitrevski, S. V. Donskov, et al., Phys. Lett. **36B**, 528, 1971.
- <sup>18</sup>S. P. Denisov, S. V. Donskov, and Yu. P. Gorin et al., Phys. Lett. **36B**, 415, 1971.
- <sup>19</sup>M. Borghini, L. Dick, J. C. Oliver, and H. Aoi et al., Phys. Lett. **36B**, 493, 1971.
- <sup>20</sup>P. Bonami and P. Borgeand et al., Nucl. Phys. **B16**, 335, 1970.
- <sup>21</sup>O. V. Dumbrais, A Compilation of Data on Real Parts of the Forward Scattering Amplitudes, JINR Preprint E2-5847, Dubna, 1971.
- <sup>22</sup>A. De Lesquen, B. Amblard, R. Bentrey, G. Cozzika, L. Bystricky, G. Deregel, Y. Ducros, J. M. Fontaine, A. Gaidot, M. Hanszouv, F. Legar, J. P. Merlo, S. Mijashita, J. Movchet, and L. Van Rossum, Measurements of Spin Rotation Parameters in Pion-Nucleon Elastic Scattering at 6 GeV/c and 16 GeV/c, Saclay Preprint, March, 1972.

Translated by J. G. Adashko  
 96